0026-895X/05/6706-1861–1873$20.00
MOLECULAR PHARMACOLOGY
Copyright © 2005 The American Society for Pharmacology and Experimental Therapeutics
Mol Pharmacol 67:1861–1873, 2005

Vol. 67, No. 6
3814/4308
Printed in U.S.A.

Corticosteroids Inhibit Cell Death Induced by Doxorubicin in Cardiomyocytes: Induction of Antiapoptosis, Antioxidant, and Detoxification Genes

Qin M. Chen, Donnia Alexander,[1] Haipeng Sun, Lifang Xie, Yan Lin, Jerome Terrand, Steve Morrissy, and Sally Purdom

Department of Pharmacology (Q.M.C., D.A., H.S., L.X., Y.L., J.T., S.M.), Interdisciplinary Graduate Program of Genetics (S.P.), University of Arizona, Tucson, Arizona

Received June 14, 2004; accepted February 17, 2005

ABSTRACT

Psychological or physical stress induces an elevation of corticosteroids in the circulating system. We report here that corticosterone (CT) protects cardiomyocytes from apoptotic cell death induced by doxorubicin (Dox), an antineoplastic drug known to induce cardiomyopathy possibly through reactive oxygen species production. The cytoprotection induced by CT is within the range of physiologically relevant doses. The lowest dose tested, 0.1 μM (or 3.5 μg/dl), inhibited apoptosis by approximately 25% as determined by caspase activity. With 1 μM CT, cardiomyocytes gain a cytoprotective effect after 8 h of incubation and remain protected for at least 72 h. Hydrocortisone, cortisone, dexamethasone, and aldosterone but not androstenedione or cholesterol also induced cytoprotection. Analyses of 20,000 gene expression sequences using Affymetrix high-density oligonucleotide array found that CT caused up-regulation of 140 genes and down-regulation of 108 genes over 1.5-fold. Among the up-regulated genes are bcl-xL, metallothioneins, glutathione peroxidase-3, and glutathione *S*-transferases. Western blot analyses revealed that CT induced an elevation of bcl-xL but not bcl-2 or proapoptotic factors bax, bak, and bad. Inhibiting the expression of bcl-xL reduced the cytoprotective effect of CT. Our data suggest that CT induces a cytoprotective effect on cardiomyocytes in association with reprogramming gene expression and induction of *bcl-xL* gene.

Stress is known to increase the level of corticosteroids in the circulating system. In humans and rodents, 1 min of psychological stress can increase the plasma corticosteroid levels by 5- to 6-fold. The neuroendocrine cascade hypothesis explains such an increase as a result of hippocampus stimulation, which in turn signals the hypothalamus to produce arginine vasopressin and corticotrophin-releasing factor, either of which can act on the anterior pituitary, causing the release of adrenocorticotropin. Adrenocorticotropin stimulates the adrenal cortex to produce corticosteroids. The major biological form of stress-induced corticosteroid is cortisol in humans and corticosterone (CT) in rodents (Guyton and Hall, 2000).

The biological function of corticosteroids has been debated over a long period. Early studies found that increased corticosteroid levels caused by long-term stress contributed to memory loss, learning disability, and damage of the hippocampus (Angelucci, 2000). Although it remains questionable whether corticosteroids damage the hippocampus, it is clear that the level of circulating corticosteroids increases with aging and Alzheimer patients have significantly elevated levels of cortisol in the ventricular cerebrospinal fluid (Angelucci, 2000). Long-term elevation of corticosteroids contributes to a number of psychiatric disorders, including posttraumatic stress disorder, depression, and dementia. In addition to the neurological impact, prolonged exposure to corticosteroids suppresses immune responses and renders individuals more susceptible to infection and inflammation.

This work was supported by National Institutes of Health grants R01-ES010826 and R01-HL076530-01, the Arizona Disease Control Research Commission, the American Heart Association, and the American Federation for Aging Research. S.P. was supported by National Institutes of Health grant T32-ES007091.

D.A., H.S., L.X., and Y.L. contributed equally to this work.

[1] Current address: Massachusetts College of Pharmacy, Boston, MA.

Article, publication date, and citation information can be found at http://molpharm.aspetjournals.org.
doi:10.1124/mol.104.003814.

ABBREVIATIONS: CT, corticosterone; Dox, doxorubicin; DMEM, Dulbecco's modified Eagle's medium; MTT, 3-[4,5-dimethylthiazol-2-yl]-2,5-diphenyl tetrazolium bromide; GST, glutathione *S*-transferase; Cox, cyclooxygenase; Hsp27, 27-kDa heat shock protein; RT-PCR, reverse transcription-polymerase chain reaction; SGK, serum/glucocorticoid-regulated kinase; β2-AR, adrenergic receptor β2; ACE1, angiotensin-converting enzyme 1; siRNA, small interference RNA; GR, glucocorticoid receptor; MF, mifepristone; ER, endoplasmic reticulum; GRE, glucocorticoid response element; PXR, pregnane X receptor; AMC, amino-4-methylcoumarin.

Despite these apparent noxious effects, corticosteroids induce the expression of gluconeogenic enzymes in the liver, the end result of which is increased fatty acid synthesis and energy storage (Guyton and Hall, 2000).

Synthetic corticosteroids have been used as pharmacological agents in several clinical applications. A few examples of synthetic forms include cortisone, dexamethasone, prednisone, and methylprednisolone. These steroids are currently used in the clinic for treatment of asthma, rheumatoid arthritis, and osteoarthritis as well as for suppression of the immune response during organ transplantation. In spite of the vast amount of information available on corticosteroid function and application, the specific effect of these steroids on the heart has not been thoroughly studied, as evidenced by the limited literature in this area.

Recent literature indicates a role of apoptosis in heart failure and various forms of heart disease (Kang and Izumo, 2000; Chen and Tu, 2002). Apoptotic-like cell death is known to play a role in cardiomyopathy induced by the antineoplastic drug doxorubicin (Dox) (Keizer et al., 1990; Singal et al., 2000). Dox is an anthracycline quinone frequently used for treatment of several types of cancer, including breast cancer and leukemia. Although Dox can be an effective antineoplastic drug, its side effect of cardiac toxicity somewhat limits its use (Keizer et al., 1990; Singal et al., 2000). The administration protocol has been improved to minimize acute cardiac toxicity. However, chronic cardiac toxicity usually develops 2 to 10 years after the drug administration, when patients can show signs of dilated cardiomyopathy, in which apoptotic-like cell death is detectable in a significant proportion of cardiomyocytes during pathological analysis of the failing hearts (Keizer et al., 1990; Singal et al., 2000).

Dox can accept electrons from oxoreductive enzymes in the mitochondria to form semiquinone free radicals, which can initiate a chain of redox reactions. Experimental data have indicated that Dox causes formation of superoxide and H_2O_2 when it is incubated with the mitochondrial fraction of heart extracts (Doroshow and Davies, 1986). In addition to inducing oxidative stress, Dox at high concentrations can interact with DNA topoisomerase, be intercalated into DNA, and cause DNA strand breaks (Singal et al., 2000). At the cellular level, Dox has often been used as a model compound for inducing apoptosis in a number of cell types, including cardiomyocytes. This provides us with an experimental system to test the effect of corticosteroids on apoptosis induced by Dox in cardiomyocytes.

Materials and Methods

Chemicals. All chemicals or drugs were obtained from Sigma-Aldrich (St. Louis, MO) unless otherwise indicated in the text.

Cell Culture and Treatment of Drugs. Cardiomyocytes were prepared from 1- to 2-day-old neonatal Sprague-Dawley rats (Harlan, Indianapolis, IN) as described previously (Coronella-Wood et al., 2004). The myocytes were seeded at a density of 2×10^6 cells per 100-mm dish, 0.3×10^6 cells per well of six-well plates, or 7.5×10^4 cells per well of 24-well plates. At 3 to 4 days after plating, cardiomyocytes were cultured in DMEM containing 0.5% fetal bovine serum and CT at 1 μM or indicated doses. At 1 to 3 days after culture with corticosteroids, media were changed to fresh DMEM containing 0.5% fetal bovine serum, and Dox was added to a final concentration of 1 μM for 20- to 24-h incubation unless otherwise indicated.

Caspase Activity Assay. Detached cells were collected by centrifugation and were mixed with adherent cells from the same well in six-well plates. The combined cells were dissolved in 200 μl of lysis buffer (0.5% Nonidet P-40, 0.5 mM EDTA, 150 mM NaCl, and 50 mM Tris, pH 7.5) for measurements of caspase-3 activity using 40 μM *N*-acetyl-Asp-Glu-Val-Asp-7-amino-4-methylcoumarin (*N*-acetyl-DEVD-AMC; Alexis Biochemicals, San Diego, CA). The released AMC was measured as the relative fluorescence unit using a 96-well fluorescence plate reader (Spectra Max; Molecular Devices, Sunnyvale, CA) with an excitation wavelength of 365 nm and an emission wavelength of 450 nm.

Annexin V Binding Assay. Cells were seeded onto coverglasses in 24-well plates. Detached cells in the supernatant were collected by 5-min centrifugation at 1000 rpm (500*g*). After washing the detached cells and adherent cells with phosphate-buffered saline separately, detached cells were combined with their corresponding group of cells remained adherent to the coverglass after addition of the labeling solution (10 mM HEPES/NaOH, pH 7.4, 140 mm NaCl, and 5 mM $CaCl_2$). Annexin V-FLOUS (Roche Diagnostics, Indianapolis, IN) was added to the sample (25 μl per well). The cells were examined under a Nikon E800m fluorescent microscope (Nikon, Tokyo, Japan), and the images were acquired using a Hamamatsu C5180 digital camera (Hamamatsu Corporation, Bridgewater, NJ) with the Adobe Photoshop software (Adobe Systems, Mountain View, CA).

MTT Assay for Cell Viability. At the end of Dox or CT plus Dox treatment, 3-[4,5-dimethylthiazol-2-yl]-2,5-diphenyl tetrazolium bromide (MTT) (Sigma-Aldrich) was added to cells in six-well plates to 0.5 mg/ml in culture medium. After 20-min incubation in a 37°C tissue culture incubator, culture medium was removed, and the resulting formazan crystals were dissolved in isopropanol. The solublized formazan products were quantified by a spectrophotometer (1601; Shimadzu, Kyoto, Japan) for absorbance at a wavelength of 570 nm. The background absorbance was subtracted by spectrophotometric measurements at a wavelength 690 nm.

Western Blot. Cells in 100-mm dishes were lysed by scraping in EB buffer (for glucocorticoid receptors, 1% Triton X-100, 10 mM Tris, pH 7.4, 5 mM EDTA pH 8.0, 50 mM NaCl, 50 mM NaF, and 2 mM Na_3VO_3) or Laemmli buffer [for bcl-2 or bcl-xL, 0.5 M Tris, pH 6.8, 2.4% (w/v) SDS, and 50% (v/v) glycerol] with freshly added protease inhibitors (Coronella-Wood et al., 2004). Protein concentration was measured by the Bradford method (Bio-Rad, Hercules, CA), the bicinchoninic acid method (Pierce Chemical, Rockford, IL), or the Warburg-Christian method (Layne, 1957). Proteins were separated by SDS-polyacrylamide gel electrophoresis and were transferred to Immobilon-P membranes (Millipore, Bedford, MA). The membrane was incubated with antibodies obtained from Cell Signaling Technology Inc. (Beverly, MA) against cytochrome *c* or caspase-3; from Santa Cruz Biotechnology, Inc. (Santa Cruz, CA) against caspase-3, glucocorticoid receptor, Bcl-xL, cyclin B1, cyclin D1, bcl-2, bax, or bak; from Sigma-Aldrich against α-smooth muscle actin, proliferating cell nuclear antigen, or vinculin; from Calbiochem (San Diego, CA) against glutathione *S*-transferase (GST)α1 or GSTmu2; from Cayman Chemical (Ann Arbor, MI) against cyclooxygenase-2 (Cox-2) and Cox-1; from Stressgen Biotechnologies (San Diego, CA) against heat shock protein 27 (Hsp27); or from MBL International (Woburn, MA) against Bad. The bound antibodies were detected using an enhanced chemiluminescence reaction after blotting with the secondary antibodies conjugated with horseradish peroxidase.

Microarray. Cardiomyocytes were harvested by TRIzol (Sigma-Aldrich) for extraction of total RNA. RNA was cleaned with an RNeasy mini kit (QIAGEN, Valencia, CA). The quality of RNA was examined by agarose gel electrophoresis and the Agilent 2100 bioanalyzer (Agilent Technologies, Palo Alto, CA) to ensure the purity and integrity of RNA suitable for microarray. The RNA was converted to cDNA by reverse transcription using the SuperScript Choice kit from Invitrogen (Carlsbad, CA) with a T7-(dT)24 primer incorporating a T7 RNA polymerase promoter. The cRNA

was prepared and labeled with biotin via in vitro transcription using the Enzo bioarray high-yield RNA transcript labeling kit (Enzo Biochemical, Farmingdale, NY). Labeled cRNA was fragmented by incubation at 94°C for 35 min. For hybridization, 15 μg of fragmented cRNA was incubated for 16 h at 45°C with a Rat Expression 230A Gene chip. After hybridization, the gene chips were automatically washed and stained with streptavidin-phycoerythrin using a fluidics station (Affymetrix, Santa Clara, CA). The probed arrays were scanned at 3-μm resolution using the Genechip System confocal scanner made for Affymetrix by Agilent Technologies. Affymetrix Microarray Suite 5.0 was used to scan and analyze the relative abundance of each gene from the average difference of intensities with p values $\leq$0.005 when perfectly matched signals are compared with mismatched signals by the Wilcoxon's signed rank test. Output data from the microarray analysis were merged with the Unigene descriptor and stored in an Excel spreadsheet. The genes reported here occurred in two independent experiments (two pairs) and at least one time during interpair comparisons. The changed p value, obtained by comparing the signals of control versus CT-treated samples using the Wilcoxon's signed rank test, is less than 0.0005 for each gene. The final data were presented as average $\pm$ S.D. obtained by intrapair and interpair comparisons. Additional statistical analyses using the unpaired Student's t tests were performed using the Stata 8.2 software from the average $\pm$ standard deviations.

RT-PCR. Total RNA extracted using TRIzol was used as templates for RT-PCR. Moloney murine leukemia virus reverse transcriptase (Invitrogen) was used for reverse transcription at 37°C for 90 min. The denaturation and primer extension temperature was 94 and 72°C, respectively. The annealing temperature varied depending on the GC content of the primers as suggested by the oligonucleotide synthesis company (Bio-Synthesis, Lewisville, TX). The primer sequences are 5′-AGGCTGGCGATGAGTTTGAA and 5′-CGGCTCTCGGCTGCTGCATT for bcl-xL, 5′-GAATTCCGTTGCTCCAGATTCACCAGATC and 5′-GAATTCTCACATGCTCGGTAGAAAACGG for metallothionein I, 5′-AAACAGGAGCCAGGCGAGAACT and 5′-CCCGTTCACATCTCCTTTCTCAAA for glutathione peroxidase-3, 5′-CCCTGAGAACCAGAGTCAGC and 5′-CCCAGCAATTCCTCATCAGT for GSTα1, 5′-ATTCGCCTGTTCCTGGAGTA and 5′-AAACGTCCACACGAATCCTC for GSTmu2, 5′-TTTTTTTTCCCAACCCTTGC and 5′-AATGAACAAAGGTTGGGGGG for serum/glucocorticoid-regulated kinase (SGK), 5-AAAGCTTGTCACTGGGGCCAGCAAA and 5′-AGGATCCAGAGCAAACTTGCTTGCA for hydroxysteroid 11β dehydrogenase 1 (11β-HSD), 5′-GAGACCCTGTGCGTGATTGC and 5′-CCTGCTCCACCTGGCTGAGG for adrenergic receptor β2 (β2-AR), 5′-TACAAGCAGTGGCAAAGGCC and 5′-CAGTATTGAGGAGAACAGATGGG for Cox-2, 5′-TAAGTACCAGGTGCTGGATGG and 5′-GGTTTCCCCTATAAGGATGAG for Cox-1, 5′-GGAGACGACTTACAGTGTAGCC and 5′-CACACCCAAAGCAATCTTC for angiotensin-converting enzyme 1 (ACE1), 5′-GAAATACACGCTCCCTCCAG and 5′-GGCTTCTACTTGGCTCCAGA for Hsp27, and 5′-AGACAGCCGCATCTTCTTGT and 5′-CCACAGTCTTCTGAGTGGCA for glyceraldehyde-3-phosphate dehydrogenase. The products were detected by agarose gel electrophoresis and ethidium bromide staining.

Bcl-xL siRNA Transfection. Primary cultured cardiomyocytes were transfected with siRNA on the third day of plating. The cells in six-well plates were incubated 6 h with 100 nM each 5′-GGCUGGCGAUGAGUUUGAAtt-3′ (abbreviated as SI; Ambion, Austin, TX) and 5′-GGUAGUGAAUGAACUCUUUtt-3′ (abbreviated as SII; Ambion) or a silencer negative control small interference RNA (siRNA) of 19-base oligonucleotide derived from a scrambled sequence (Ambion) in a 1-ml mixture of Opti-MEM (Invitrogen) and DMEM containing 3 μl of Oligofectamine (Invitrogen). At 48 h after transfection, cells were treated with corticosterone for determining the protein level of bcl-xL and the effect of corticosterone on Dox-induced apoptosis.

Results

Corticosterone Inhibits Apoptosis Induced by Dox. Cardiomyocytes are adherent cultures, but they detach and round up when they undergo apoptosis. Such morphology was observed with the treatment of Dox at 1 μM or higher doses. Caspase-3 activity measurement was used as a quantitative assay for apoptosis. When cardiomyocytes were incubated with Dox for 24 h, an elevated activity of caspase-3 was observed with Dox at 0.1 μM or above (Fig. 1). Caspase-3 activity assay indicates that 1.0 μM was an appropriate dose for inducing apoptosis because a higher dose (5.0 μM) did not seem to induce more caspase-3 activity (Fig. 1A). Activation of caspase-3 by Dox was detectable at 9 h but reached the highest level at 24 h (Fig. 1B).

The vast amount of literature concerning CT involves induction of apoptosis in lymphocytes and neuronal cells. We have tested whether CT could induce apoptosis in cardiomyocytes. Our experiments failed to show that CT induced apoptosis in cardiomyocytes using physiologically relevant doses (0.1 μM or 3.5 μg/dl to 1 μM or 35 μg/dl) or higher (1–100 μM). To test the effect of CT on Dox-induced apoptosis, cardiomyocytes were cultured in medium containing 1.0 μM CT for 3 days and were placed in fresh medium afterward for Dox treatment. Figure 1B shows that cells cultured with CT were reluctant to activate caspase-3 as evidenced by measurements at various times after Dox treatment. The effect of CT was dose-dependent and the lowest dose tested, 0.1 μM, showed approximately 25% protective effect (Fig. 1C). CT at 1 μM can inhibit approximately 70% of caspase-3 activity induced by Dox (Fig. 1C).

Morphological analysis was consistent with caspase-3 mea-

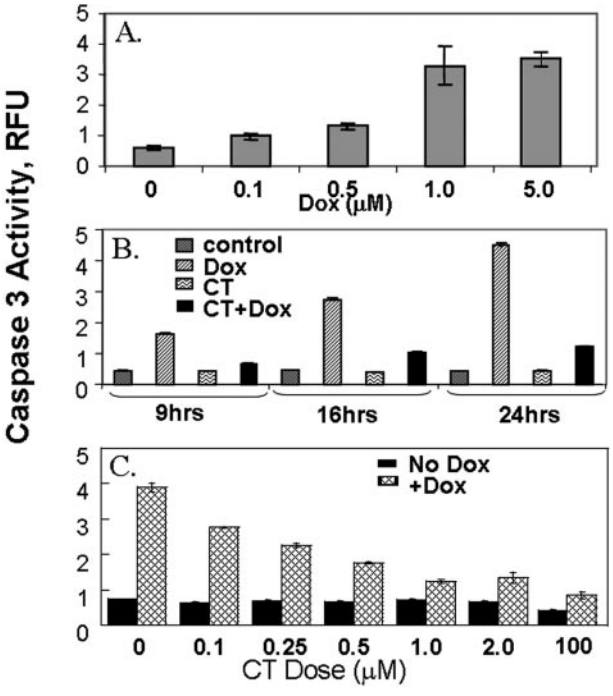

Fig. 1. CT pretreatment inhibits caspase activation induced by Dox. Cardiomyocytes were treated with Dox at indicated doses (A). For pretreatment of CT, cardiomyocytes were cultured in DMEM containing 1 μM (B) or various concentrations of CT for 3 days (C). After replacing the cells with fresh medium, cells were treated with 1 μM Dox for 24 h (A and C) or various times (B) before harvesting for measurement of caspase-3 activity using DEVD-AMC as a substrate.

surements, showing that CT pretreatment prevented cells from detaching and presumably undergoing apoptosis (Fig. 2, A–D). In addition to morphological changes and activation of caspases, apoptosis can be measured by Annexin V binding. Using Annexin V conjugated with the fluorescein isothiocyanate fluorescent group, we found that Dox induced binding of Annexin V (Fig. 2, E and F). Culturing cardiomyocytes with CT prevented Dox from inducing Annexin V binding (Fig. 2, G and H). Propidium iodine stains nuclei, allowing us to examine the nuclear morphology of cells treated with Dox (Fig. 2, I and J). Scoring the percentage of cells that round up and detach or exhibit the nuclear morphology of apoptotic cells (Chen et al., 2002) provided quantitative evidence that CT pretreatment indeed inhibits Dox from inducing apoptotic-like cell death (Fig. 2K). To demonstrate that CT indeed prevented the loss of cell viability induced by Dox, we measured cell viability using MTT assay. Figure 2L shows that whereas Dox caused reduction in cell viability, treatment of CT prevented the loss of cell viability. Additional evidence supporting CT inhibition of apoptosis was shown with the DNA degradation assay (Fig. 3A), loss of mitochondrial cytochrome *c* (Fig. 3B), and caspase-3 cleavage (Fig. 3C).

Cell death can be induced by a number of damaging agents. To address whether CT inhibits apoptosis induced by chemicals in addition to Dox, we tested the effect of CT on caspase-3 activated by two other cardiac toxins: palmitate and 2-deoxyglucose (De Windt et al., 2000; Hickson-Bick et al., 2002). Although it is not clear whether oxidative stress

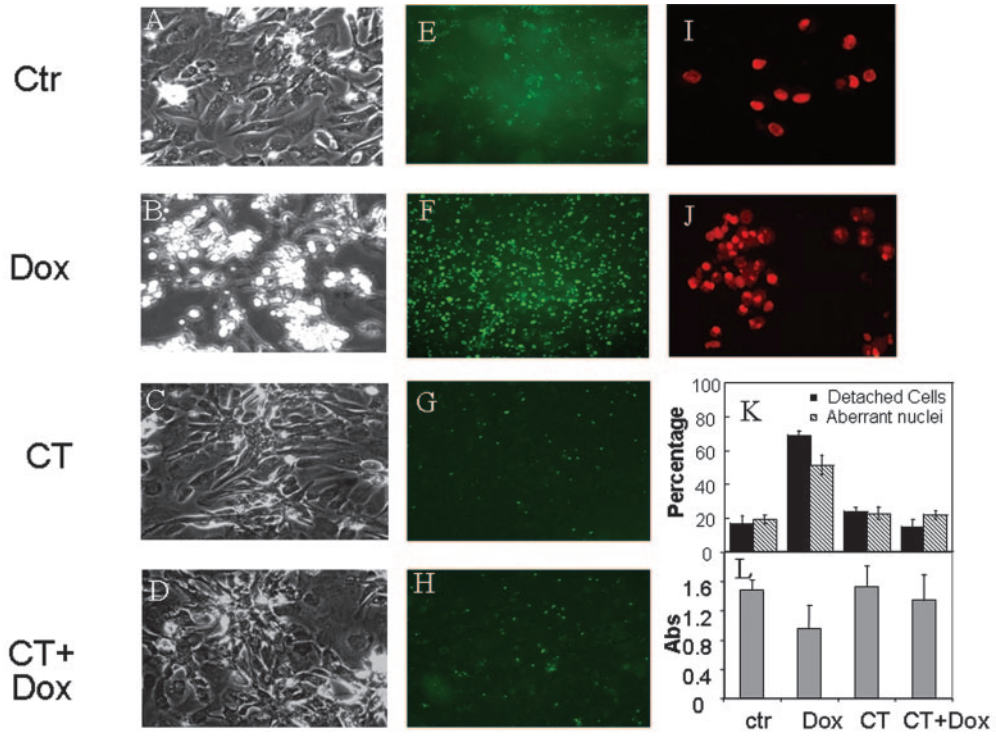

Fig. 2. Morphological evidence, Annexin V binding assay, and staining of nuclei indicate that CT induces cytoprotective response. Cardiomyocytes were cultured in DMEM containing 1 μM CT for 3 days. The cells were then placed in fresh medium and treated with 1 μM Dox for 24 h. The morphology was recorded under an Olympus phase contrast microscope with 20× lens (A–D). For Annexin V staining, cardiomyocytes were grown on coverglasses in 24-well plates. Annexin V-fluoresein isothiocyanate-positive cells were recorded under a Nikon fluorescence microscope with 10× lens (E–H). Control (I) or cells floated after Dox treatment (J) were collected for staining of nuclei with low concentration of propidium iodine (1.0 μg/ml) as described in Chen et al. (2002). The percentage of cells floated into the medium or the percentage nuclei showed nuclear condensation or fragmentation (K) was scored under a microscope as described previously (Chen et al., 2002). For cell viability assay (L), MTT was added to cells for 20-min incubation as described under *Materials and Methods*, and the data of absorbance represent mean ± S.D. from three independent experiments.

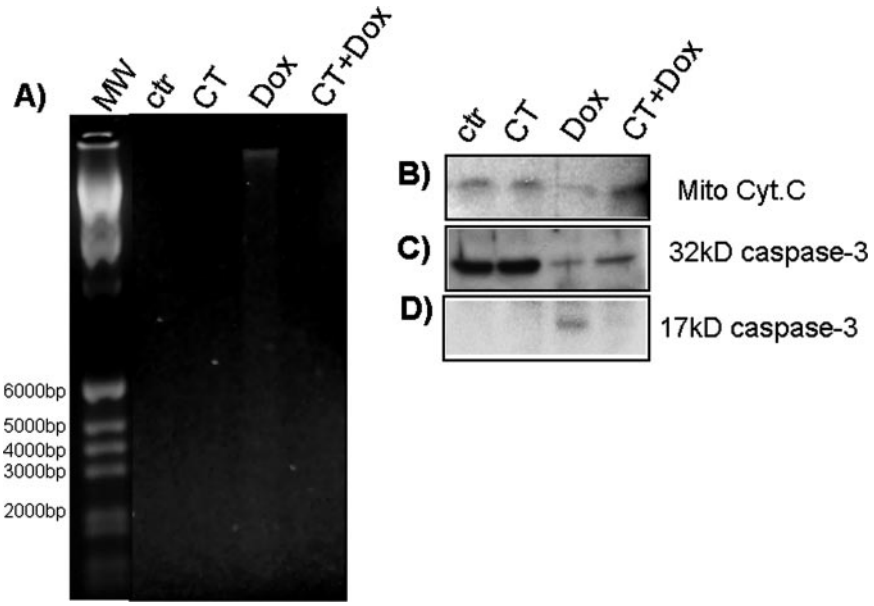

Fig. 3. Assays of DNA degradation, mitochondrial loss of cytochrome *c*, and cleavage of caspase-3 support that CT induces cytoprotection. Cardiomyocytes were cultured in DMEM containing 1 μM CT for 3 days. The cells were placed in fresh medium and treated 24 h with 1 μM Dox for measurement of DNA degradation (A) by agarose gel electrophoresis after extracting genomic DNA as described previously (Chen et al., 1995) and for measurement of mitochondrial cytochrome *c* (B) or intact (C) versus cleaved (D) caspase-3 by Western blot as described under *Materials and Methods*.

plays a role in palmitate or 2-deoxyglucose toxicity, these two compounds induced activation of caspase-3 at 0.5 and 25 mM doses, respectively (Fig. 4A). Pretreatment with CT prevented palmitate or glutamate from inducing caspase-3 activation (Fig. 4A), suggesting that CT may protect cardiomyocytes from cell death induced by a number of toxins.

We then tested the effect of several different corticosteroids on caspase-3 activation induced by Dox to determine whether the inhibition of apoptosis is limited to CT. Among the steroids tested, hydrocortisone, dexamethasone, cortisone, and aldosterone showed an inhibitory effect against Dox-induced caspase-3 activation (Fig. 4B). 4-Androstenedione, an intermediate of steroid synthesis, and cholesterol, the precursor of adrenal steroids, failed to inhibit caspase-3 activation (Fig. 3B).

Delayed Time Course and Dependence on Receptor and Protein Synthesis. To determine the mechanism of CT-induced cytoprotection, we tested the role of the glucocorticoid receptor (GR) (Yudt and Cidlowski, 2002). Rat neonatal cardiomyocytes express GR, and the two protein bands from Western blot analyses represent the 94-kDa α isoform and 90-kDa β isoform (Fig. 5A). Treatment of CT did not seem to alter the level of GRs (Fig. 5A). Mifepristone (MF) can bind to GR with high affinity and maintains the receptor in an inappropriate conformation for corticosteroid binding (Cadepond et al., 1997). We tested the effect of MF on CT-induced cytoprotection by pretreating cells with MF for 30 min before CT addition. It was found that CT in the presence of MF could no longer inhibit caspase-3 activation induced by Dox treatment (Fig. 5B).

The cytoprotective effect of CT was first discovered by culturing cardiomyocytes with CT for 3 days. To define the minimal time frame required for CT to produce a cell survival response, we pretreated cells with CT from 30 min to 8 h or for 1, 2, and 3 days before Dox treatment. The results showed that 8-h CT pretreatment was starting to have a cytoprotective effect (Fig. 6A), and 24-h pretreatment was just as effective as 3-day pretreatment in inhibiting apoptosis (Fig. 6B). The fact that CT requires 8 h or more to induce a cell survival response led us to postulate that new protein synthesis could have played a role. We therefore tested the dependence of new protein synthesis on CT-induced cell survival by placing cells in a medium deficient of the essential amino acids methionine and cysteine or by adding the protein synthesis inhibitor cycloheximide to the complete culture medium during 24-h CT pretreatment. The culture medium was changed back to fresh complete medium during 24-h Dox treatment. In complete medium, CT inhibited 76.2% caspase activity induced by Dox treatment. The methionine- and cysteine-deficient medium reduced CT inhibition to 48.1%. Addition of 0.5 μg/ml cycloheximide during CT pretreatment reduced the protective effect down to 20%. The results indicate a role of new protein synthesis in CT-induced cell survival response.

Gene Expression Altered by Corticosteroids. Microarray analysis allows us to systematically address the mechanism of CT-induced cytoprotection without the bias of prior knowledge. We have used the Affymetrix high-density oligonucleotide expression array system to identify the genes that change expression levels by CT treatment. RNA was harvested from control or treated cardiomyocytes at 24 h after addition of 1 μM CT. This time was chosen

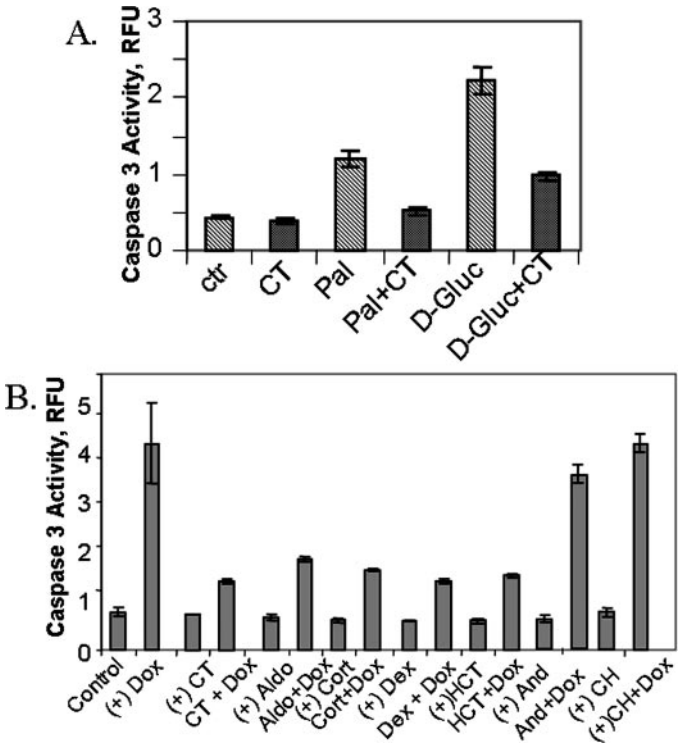

Fig. 4. CT inhibits palmitate and D-glucose from activating caspases and effect of various steroids. Cardiomyocytes were cultured 3 days in DMEM containing 1 μM CT (A and B), aldosterone (Aldo, 1 μM), cortisone (Cort, 1 μM), dexamethasone (Dex, 1 μM), hydrocortisone (HCT, 1 μM), 4-androsterendione (And, 1 μM), or cholesterol (CH, 10 μM; B). The cells were then placed in fresh medium for 24-h treatment with 0.5 mM palmitate (Pal), 25 mM D-glucose (A), or 1 μM Dox (B). Cells were harvested for measurement of caspase-3 as described under *Materials and Methods*.

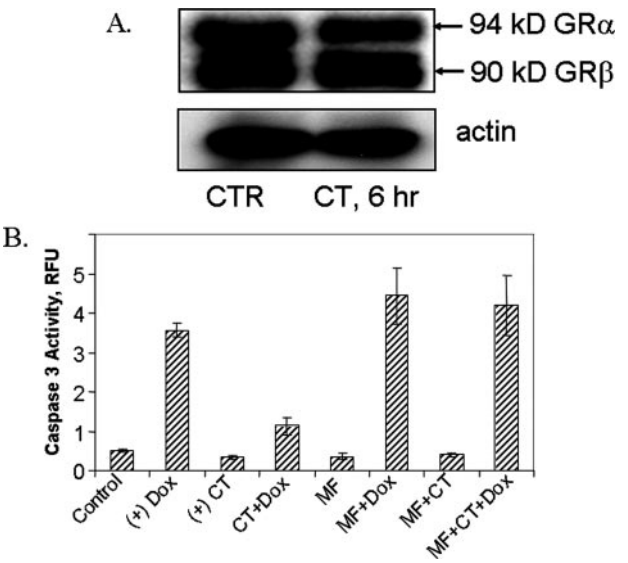

Fig. 5. Role of GR in CT-induced cell survival response. Cardiomyocytes were treated with 1 μM CT for 6 h before harvesting for measurement of GR using Western blot (20 μg of protein/lane, A). Smooth muscle α actin blotting was included as a loading control (A). For measurement of caspase-3, 1 μM MF was added to the indicated group 30 min before addition of 1 μM CT (B). Cells were cultured in the medium containing CT in the presence or absence of MF for 3 days (B). Cells were placed in fresh medium for 24-h treatment with 1 μM Dox (B).

TABLE 1

Gene expression profile of cardiomyocytes treated with corticosterone

Cardiomyocytes were treated with 1 μM CT for 24 h and were harvested for microarray analyses as described under *Materials and Methods*. The Wilcoxon's signed rank test in the Microarray Suite 5.0 selected the genes that show increases or decreases by CT treatment with p value <0.005 during intrapair comparisons. The data represent mean ± S.D. of -fold changes from intra- and interpair comparisons. Additional statistical analysis using Stata 8.2 Student's t test confirmed the significant differences with $p \leq 0.05$ (indicated by *) or $p \leq 0.01$ (no indication) when CT-treated samples were compared with control untreated samples. Down-regulated genes are indicated in italics, within the same category of up-regulated genes.

Antioxidant/detoxification enzymes/metal binding protein		
Rn0.1491	Glutathione peroxidase-3	1.92 ± 0.30
Rn0.10460	Glutathione *S*-transferase, α1	2.07 ± 0.37
Rn0.625	Glutathione *S*-transferase, μ type 2	1.80 ± 0.07
Rn0.7854	Microsomal glutathione *S*-transferase 2	1.92 ± 0.36
Rn0.867	Flavin-containing monooxygenase 1	2.59 ± 0.52
Rn0.11676	Flavin-containing monooxygenase 3	111.63 ± 57.78*
Rn0.26060	Cytochrome P450 2d18	2.15 ± 0.22
Rn0.1507	Aryl sulfotransferase	6.34 ± 1.04
Rn0.19540	diacetyl/l-xylulose reductase	3.30 ± 0.70
Rn0.54397	metallothionein	5.44 ± 0.99
Rn0.64596	metallothionein-II	5.39 ± 1.28
Rn0.91296	Transferrin	4.43 ± 2.17*
Rn0.32777	Ceruloplasmin	2.15 ± 0.12
Rn0.1451	Selenoprotein P, plasma, 1	2.45 ± 0.66*
Antiapoptosis		
Rn0.10323	bcl-xl	1.81 ± 0.27
Muscle or contractile proteins		
Rn0.40120	Fast myosin alkali light chain	4.47 ± 0.64
Rn0.48663	Myosin heavy chain 7	1.67 ± 0.13
Rn0.94969	Myosin heavy chain 11	2.30 ± 0.54*
Rn0.27152	α-Dystrobrevin	2.36 ± 0.37
Rn0.6303	Muscle ring finger protein 1	2.84 ± 0.23
Rn0.22171	Cypher (PDZ-LIM domain Z-line protein)	1.57 ± 0.11
Channel protein		
Rn0.1618	Aquaporin 1	3.15 ± 0.28
Rn0.3205	Glucose transporter 1	1.97 ± 0.13
Rn0.1314	Glucose transporter 4	2.02 ± 0.29
Rn0.67076	Organic anion transporter 10	1.79 ± 0.19
Rn0.10047	Potassium inwardly-rectifying channel J(5)	1.59 ± 0.06
Rn0.88300	Gap junction membrane channel protein α 5	2.61 ± 0.37
Rn0.87329	*Na^+/K^+ ATPase α3 subunit*	*0.52 ± 0.10*
Rn0.839	*FXYD domain-containing ion transport regulator 6*	*0.65 ± 0.03*
Rn0.32566	*Fatty acid binding protein 3*	*0.50 ± 0.07*
Prostaglandin synthesis		
Rn0.44404	Prostaglandin-endoperoxide synthase 1 (Cox1)	3.92 ± 0.78
Rn0.44369	Prostaglandin-endoperoxide synthase 2 (Cox2)	3.62 ± 0.32
Rn0.10498	Prostaglandin I2 synthase	2.08 ± 0.28
Rn0.11400	Prostaglandin D synthase	2.02 ± 0.39*
Endocrine factors or their binding proteins		
Rn0.2490	Interleukin 15	1.87 ± 0.19
Rn0.4256	Vascular endothelial growth factor D	2.02 ± 0.34
Rn0.8037	Epidermal growth factor-like protein, T16	3.10 ± 0.78*
Rn0.6282	Insulin-like growth factor 1	2.20 ± 0.60*
Rn0.29042	Nephroblastoma overexpressed gene (NOV)	1.71 ± 0.12
Rn0.8929	Galanin	4.40 ± 1.40*
Rn0.10232	Adrenomedullin	2.29 ± 0.41
Rn0.90931	Bone morphogenetic protein 2	2.30 ± 0.13
Rn0.40476	Bone morphogenetic protein 6	1.63 ± 0.09
Rn0.22500	Follistatin	1.63 ± 0.09
Rn0.48835	Follistatin-like 3	2.3 ± 0.00
Rn0.6431	Insulin-like growth factor-binding protein 6	2.13 ± 0.46*
Rn0.1664	*Angiopoietin-like 2*	*0.37 ± 0.15*
Rn0.9714	*Neuropeptide Y*	*0.52 ± 0.13*
Rn0.4772	*Small inducible cytokine A2*	*0.51 ± 0.18*
Rn0.1593	*Insulin-like growth factor-binding protein 5*	*0.36 ± 0.05*
Receptors		
Rn0.10206	Adrenergic receptor-β2	2.85 ± 0.95*
Rn0.10294	Serotonin receptor 2A	2.21 ± 0.62*
Rn0.4102	Endothelial differentiation sphingolipid G protein-coupled receptor 1	2.29 ± 0.85*
Rn0.11200	Endothelial differentiation lysophosphatidic acid G protein-coupled receptor 2	2.65 ± 0.34
Rn0.1820	Peripheral benzodiazepine receptor	1.80 ± 0.32*
Rn0.9962	Thyrotropin releasing hormone receptor	1.76 ± 0.34*
Signaling molecules		
Rn0.4636	Serum/glucocorticoid regulated kinase	2.88 ± 0.19
Rn0.6343	Serine threonine kinase pim3	2.14 ± 0.41
Rn0.6890	Ras like protein	3.38 ± 0.40
Rn0.6500	G protein-coupled receptor kinase 5	1.75 ± 0.14
Rn0.42890	cAMP-regulated guanine nucleotide exchange factor II	2.40 ± 0.62*
Rn0.9983	Protein kinase A anchor protein 5	2.01 ± 0.28
Rn0.9791	Insulin receptor substrate 3	1.71 ± 0.12
Rn0.10696	Phosphatidylserine-specific phospholipase A1	2.14 ± 0.00

TABLE 1
Continued

Rn0.37601	myo-Inositol 1-phosphate synthase A1	11.64 ± 8.30*
Rn0.10239	FMS-like tyrosine kinase 1	1.93 ± 0.32
Rn0.7492	Protein tyrosine phosphatase-like protein PTPLB	1.98 ± 0.30
Rn0.31120	Nonreceptor protein tyrosine phosphatase 16	1.75 ± 0.22
Rn0.7274	Enigma (PDZ-LIM domain protein)	1.79 ± 0.26
Rn0.17933	Enigma homolog	1.63 ± 0.20
Rn0.24612	Arg/Abl-interacting protein ArgBP2	1.67 ± 0.18
Rn0.19950	*Rac GTPase-activating protein 1*	*0.29 ± 0.09*
Rn0.12100	*Serum-inducible kinase*	*0.52 ± 0.07*
Rn0.10865	*Serine/threonine kinase 12*	*0.53 ± 0.04*
Rn0.14848	*Protein kinase Sak-a*	
Rn0.28232	*Maternal embryonic leucine zipper kinase*	*0.45 ± 0.04*
Rn0.11034	*Polo-like serine/threonine protein kinase*	*0.55 ± 0.09*
Rn0.91	*CDC28 protein kinase 1*	*0.65 ± 0.03*
Rn0.22271	*Nonreceptor protein-tyrosine-phosphatase 3*	*0.56 ± 0.06*
Rn0.44437	*Protein phosphatase 2A regulatory subunit B*	*0.43 ± 0.04*
Rn0.12679	*Acid sphingomyelinase-like phosphodiesterase 3b*	*0.60 ± 0.07*
Transcription factors		
Rn0.6211	Glucocorticoid-induced leucine zipper	2.57 ± 0.37
Rn0.12550	Nuclear factor-κB inhibitor α (IκBα)	2.31 ± 0.23
Rn0.6479	CCAAT/enhancer binding protein β	1.81 ± 0.16
Rn0.6975	CCAAT/enhancer binding protein δ	1.60 ± 0.18
Rn0.19481	Kruppel-like factor 9	2.82 ± 0.54
Rn0.95264	Kruppel-like factor 13	1.79 ± 0.19
Rn0.24978	Kruppel-like factor 15	3.52 ± 0.56
Rn0.1671	Epicardin (Pod1)	1.55 ± 0.06
Rn0.15099	*Transcription factor SOX4*	*0.39 ± 0.04*
Rn0.3227	*Forkhead related transcription factor 10*	*0.52 ± 0.07*
Rn0.15992	*Lactose operon repressor*	*0.46 ± 0.13*
Rn0.9027	*Enhancer of zeste homolog 2 (ENX-1)*	*0.56 ± 0.10*
Rn0.93372	*Sry-related HMG-box protein Sox11*	*0.46 ± 0.02*
Chromatin or DNA binding proteins		
Rn0.8353	Histone H2A0.1	1.85 ± 0.40*
Rn0.82737	Zinc finger protein 36 (TIS11)	1.87 ± 0.19
Rn0.3053	SWI/SNF-related actin-dependent chromatin regulator d(2)	1.89 ± 0.34
Rn0.3636	*H2A histone family member Z*	*0.58 ± 0.02*
Rn0.27469	*Histone H1-binding protein*	*0.66 ± 0.00*
Rn0.2874	*High mobility group box 2*	*0.53 ± 0.05*
Rn0.3517	*High mobility group protein 17*	*0.59 ± 0.05*
Rn0.33226	*Mini chromosome maintenance deficient 6*	*0.47 ± 0.10*
Rn0.113	*Mini chromosome maintenance deficient 7*	*0.63 ± 0.04*
Rn0.37193	*Small nuclear ribonucleoprotein D*	*0.56 ± 0.06*
Rn0.25771	*Heterogeneous nuclear ribonucleoprotein A1*	*0.63 ± 0.05*
Rn0.7870	*Chromosome condensation-related SMC-associated protein 1*	*0.56 ± 0.05*
Cytosketetal proteins		
Rn0.69726	Integrin α8	1.81 ± 0.16
Rn0.82732	Actin α1	2.38 ± 0.42
Rn0.958	Actin γ2	1.63 ± 0.11
Rn0.52763	Ankyrin 3	1.59 ± 0.06
Rn0.1657	Desmin	2.80 ± 0.42
Rn0.46362	Desmuslin	2.31 ± 0.66*
Rn0.22906	Fibrillin-2	2.35 ± 0.25
Rn0.19032	Microtubule-associated protein 1b	1.63 ± 0.09
Rn0.39792	Melusin 2 (integrin β1 binding protein)	2.23 ± 0.20
Rn0.91044	*Integrin α1*	*0.55 ± 0.15*
Rn0.40800	*Tubulin, β15*	*0.60 ± 0.05*
Rn0.8216	*Tubulin, β3*	*0.48 ± 0.17*
Rn0.2458	*Tubulin, β5*	*0.59 ± 0.02*
Rn0.45205	*Kinesin-like 7*	*0.39 ± 0.04*
Rn0.38181	*Kinesin-related protein*	*0.47 ± 0.00*
Rn0.11104	*Acidic keratin complex 1 gene 18*	*0.44 ± 0.20*
Rn0.3515	*Profilin II*	*0.55 ± 0.08*
Rn0.555	*Stathmin 1*	*0.40 ± 0.05*
Cell surface and extracellular matrix protein		
Rn0.13593	Laminin α-5 chain	1.80 ± 0.32
Rn0.2029	Syndecan 4	1.88 ± 0.26
Rn0.30124	Osteomodulin	2.06 ± 0.35
Rn0.92160	C-CAM4 protein	1.59 ± 0.06
Rn0.13805	Podocalyxin-like	3.78 ± 1.03
Rn0.65510	Proline arginine-rich end leucine-rich repeat protein	1.66 ± 0.15
Rn0.17364	Heparan sulfate 3-*O*-sulfotransferase 1	3.96 ± 1.03
Rn0.11362	*Lamin B1*	*0.48 ± 0.03*
Rn0.11176	*Syndecan 1*	*0.62 ± 0.00*
Rn0.11127	*Syndecan 2*	*0.56 ± 0.06*
Rn0.13741	*Leprecan*	*0.65 ± 0.03*
Rn0.35666	*Versican*	*0.58 ± 0.10*
Rn0.82724	*Thymus cell surface antigen*	*0.65 ± 0.03*

TABLE 1
Continued

Rn0.8396	*Dermatopontin*	*0.41 ± 0.24**
Rn0.7350	*Fibrulin-2 precursor*	*0.54 ± 0.09*
Rn0.12723	*Tenascin*	*0.38 ± 0.09*
Energy metabolism enzymes		
Rn0.4212	6-Phosphofructokinase	2.41 ± 1.15*
Rn0.7686	β-Galactosidase, α peptide	1.96 ± 0.16
Rn0.17661	*L-arginine:glycine amidinotransferase*	*0.48 ± 0.07*
Rn0.35508	*Phosphoenolpyruvate carboxylase*	*0.59 ± 0.07*
Rn0.3519	*Malic enzyme 1*	*0.59 ± 0.05*
Rn0.4227	*Mitochondrial SCO2 protein homolog*	*0.57 ± 0.04*
Rn0.40511	*Myoglobin*	*0.41 ± 0.16*
Lipid/steroid metabolism		
Rn0.29594	HMG-CoA synthase 2	7.59 ± 5.04*
Rn0.888	Hydroxysteroid 11-β dehydrogenase 1	3.51 ± 0.50
Rn0.24825	Farnesyl-pyrophosphate synthetase	2.48 ± 0.35
Rn0.80832	Phytanoyl-CoA hydroxylase	1.60 ± 0.05
Rn0.2856	Carnitine palmitoyltransferase 1	1.81 ± 0.42*
Rn0.1023	*Stearoyl-coenzyme A desaturase 1*	*0.42 ± 0.21*
Amino acid and protein synthesis or modification		
Rn0.2204	Glutamine synthetase 1	2.93 ± 0.65
Rn0.3066	5-Oxoprolinase	1.59 ± 0.13
Rn0.2589	Cytosolic cysteine dioxygenase 1	2.04 ± 0.48*
Rn0.95333	Ribosomal protein L22	1.81 ± 0.25
Rn0.10958	Eukaryotic elongation factor 2 kinase	2.73 ± 0.99*
Rn0.6299	Pyridoxine 5-phosphate oxidase	2.02 ± 0.35
Rn0.10	Tissue-type transglutaminase	2.29 ± 0.46
Rn0.14865	*Cysteine-tRNA ligase*	*0.53 ± 0.09*
Rn0.14939	*Tryptophan-tRNA ligase α-2 chain*	*0.63 ± 0.05*
Rn0.30218	*Phosphoserine aminotransferase*	*0.60 ± 0.05*
Rn0.3148	*δ1-Pyrroline-5-carboxylate synthetase*	*0.59 ± 0.02*
Rn0.11172	*Asparagine synthetase*	*0.54 ± 0.04*
Protease or protease inhibitor		
Rn0.10149	Angiotensin 1-converting enzyme 1	5.21 ± 2.67*
Rn0.11347	Cathepsin S	1.91 ± 0.22
Rn0.956	Cystatin C	1.94 ± 0.17
Rn0.6051	Dipeptidase 1	4.01 ± 0.32
Rn0.7897	Disintegrin and metalloproteinase with thrombospondin motifs 1	1.79 ± 0.19
Rn0.7866	Autophagy-related cysteine endopeptidase 2	1.82 ± 0.30
Rn0.3467	Tissue inhibitor of metalloproteinase 3	3.64 ± 0.60
Rn0.128	Serine protease inhibitor 3	4.28 ± 1.91*
Rn0.780	α-2-Macroglobulin (proteinase inhibitor)	2.02 ± 0.32
Rn0.2862	*Calpain 6*	*0.40 ± 0.05*
Rn0.16195	*Caspase 11*	*0.58 ± 0.03*
Rn0.81078	*Caspase 12*	*0.63 ± 0.05*
Rn0.33193	*Matrix metalloproteinase 12*	*0.38 ± 0.05*
Rn0.3102	*Ubiquitin conjugating enzyme E2C*	*0.35 ± 0.07*
Rn0.12053	*Ubiquitin thiolesterase 1*	*0.61 ± 0.05*
Stress genes		
Rn0.3841	27-kDa Heat shock protein 1	1.79 ± 0.19
Rn0.3201	20-kDa Heat shock protein	1.75 ± 0.22
Rn0.11183	*DNA-damage inducible transcript 3*	*0.62 ± 0.05*
Rn0.7102	*T-complex-type molecular chaperone (TCP-1)*	*0.47 ± 0.17*
Rn0.23638	*Radiation-inducible immediate-early gene IEX-1*	*0.59 ± 0.08*
Cell cycle regulators		
Rn0.96088	p57kip2	7.10 ± 0.46
Rn0.3504	Rgc32 protein (activator of p34CDC-2 kinase)	2.84 ± 0.29
Rn0.44920	Quiescin Q6	1.97 ± 0.13
Rn0.52228	Growth arrest-specific 6	2.07 ± 0.68*
Rn0.9232	*Cyclin B1*	*0.42 ± 0.03*
Rn0.96083	*Cyclin D2*	*0.59 ± 0.05*
Rn0.6934	*Cdc2 homolog A*	*0.27 ± 0.02*
Rn0.25026	*CDK2-associated dual specificity phosphatase*	*0.35 ± 0.10*
Rn0.48717	*CDK inhibitor 2A*	*0.59 ± 0.02*
Rn0.6116	*Cell division control protein CKS2*	*0.33 ± 0.05*
Rn0.223	*Proliferating cell nuclear antigen (PCNA)*	*0.59 ± 0.04*
Rn0.12774	*Cell proliferation antigen Ki-67*	*0.23 ± 0.01*
Rn0.40389	*p32-Subunit of replication protein A*	*0.63 ± 0.05*
Rn0.12916	*Replication licensing factor MCM3*	*0.51 ± 0.05*
Rn0.8341	*Replication licensing factor MCM4*	*0.52 ± 0.06*
Rn0.17046	*Replication factor C 37-kDa subunit*	*0.60 ± 0.06*
Rn0.3711	*Replication factor C 38-kDa subunit*	*0.53 ± 0.10*
Rn0.22094	*Ribonucleoside-diphosphate reductase M1*	*0.47 ± 0.02*
Rn0.90996	*DNA topoisomerase 2α*	*0.28 ± 0.07*
Rn0.4191	*Thymidine kinase 1*	*0.50 ± 0.06*
Rn0.92497	*DNA polymerase α subunit IV (primase)*	*0.63 ± 0.05*
Rn0.30660	*Anaphase-promoting complex subunit 8*	*0.29 ± 0.05*
Rn0.3246	*Gene rich cluster C8 gene*	*0.47 ± 0.00*

TABLE 1
Continued

Rn0.24582	*Extra spindle poles like 1*	*0.32 ± 0.13**
Rn0.9262	*Cell cycle protein p55CDC*	*0.53 ± 0.04*
Cytokines		
Interleukin 15		1.87 ± 0.19
Miscellaneous		
Rn0.4086	Tensin	2.11 ± 0.45*
Rn0.3790	cd36 Antigen (fatty acid binding/transport protein)	1.72 ± 0.25
Rn0.1231	CD59 antigen	1.66 ± 0.17
Rn0.10994	EGL nine homolog 3	2.10 ± 0.44*
Rn0.1256	Lipocalin 7	1.79 ± 0.19
Rn0.10295	Orosomucoid 1	11.40 ± 3.69
Rn0.94754	Cysteine-rich protein 2	1.90 ± 0.12
Rn0.11345	Cysteine-rich protein 3	1.94 ± 0.45*
Rn0.3407	*N*-myc downstream-regulated gene 2	1.94 ± 0.22
Rn0.9453	Fracture callus protein MUSTANG	2.42 ± 0.16
Rn0.9763	Prostatic steroid-binding protein 1	2.61 ± 0.78*
Rn0.54473	Enzymatic glycosylation-regulating gene	2.20 ± 0.17
Rn0.27923	B-cell translocation gene 2 (NGF inducible)	2.37 ± 0.98*
Rn0.4346	Late gestation lung protein 1	3.26 ± 0.37
Rn0.3464	D-Dopachrome tautomerase	1.67 ± 0.18
Rn0.11984	*Melanoma antigen, family D, 2*	*0.45 ± 0.06*
Rn0.271	*Pituitary tumor-transforming 1*	*0.45 ± 0.07*
Rn0.902	*Retinol-binding protein 1*	*0.59 ± 0.04*
Rn0.9727	*Pancreatitis-associated protein*	*0.31 ± 0.06*
Rn0.43122	*Trophoblast glycoprotein*	*0.58 ± 0.03*
Rn0.7085	*Antigen identified by monoclonal antibody MRC OX-2*	*0.32 ± 0.14*
Rn0.37141	*Neuronal olfactomedin-related ER localized protein*	*0.56 ± 0.09*
Rn0.39396	*Transforming acidic coiled-coil containing protein 3*	*0.47 ± 0.03*
Rn0.3169	*Neural precursor cell expressed, developmentally down-regulated gene 4A*	*0.29 ± 0.06*
Rn0.42929	*Cysteine knot superfamily 1, bone morphogenic protein antagonist 1*	*0.60 ± 0.06*
Rn0.16593	*Esophageal cancer related gene 4*	*0.60 ± 0.05*
Rn0.34087	*Exportin 1*	*0.60 ± 0.11*
Rn0.9190	*Brain expressed X-linked 2*	*0.47 ± 0.08*
Rn0.91636	*Glycosyltransferase AD-017*	*0.62 ± 0.04*
Rn0.8430	*Immunoglobulin superfamily containing leucine-rich repeat*	*0.58 ± 0.08*
Rn0.10072	*Interleukin 1 receptor-like 1*	*0.45 ± 0.16*

based on the studies of the apoptosis time course showing that the cells had gained maximal cytoprotective capacity. We examined the expression of 20,000 genes or transcribed sequences using the Rat Expression 230A Gene chips. The results revealed that approximately 1.7% genes changed expression by 1.5-fold or more in cells treated with CT. CT induced 140 genes plus 116 unnamed transcribed sequences to increase their expression more than 1.5-fold. There were 108 genes plus 72 unnamed transcribed sequences down-regulated by CT treatment. The unnamed transcribed sequences have been verified by searching against the Unigene database (http://www.ncbi.nlmr.gov) for gene names and have either no sequence homology or less than 50% homology to a specific gene in the database. Table 1 lists the genes that are up- or down-regulated by CT treatment. We have verified the gene array data by RT-PCR analysis for 12 genes. All of the genes tested by RT-PCR were up-regulated by CT treatment (Fig. 7). The RT-PCR data are therefore consistent with the microarray finding.

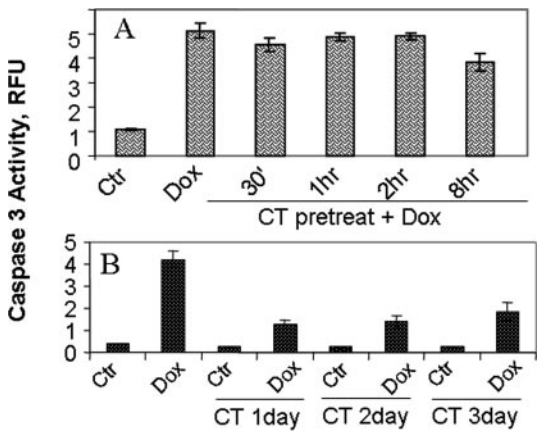

Fig. 6. Time required for CT to induce cell survival response. Cardiomyocytes were treated with 1 μM CT for indicated time (A) before being placed in fresh medium for 24 h treatment with 1 μM Dox (B). At the end of treatment, cells were harvested for measurement of caspase-3 activity as described under *Materials and Methods*.

Among the up-regulated genes found by microarray analyses are the antiapoptotic gene bcl-xL and several antioxidant, detoxification enzymes and metal binding proteins, including metallothionein I and II, glutathione peroxidase-3, and glutathione *S*-transferases (Table 1). In addition, a number of the genes up-regulated by CT have been shown to contribute to cell survival in the literature, some of which have been shown specifically to be cytoprotective for cardiomyocytes. These genes include insulin like growth factor-1, Hsp27, prostaglandin-endoperoxide synthetase-2 (Cox-2), and SGK (Table 1). Microarray analyses also revealed that CT induced six muscle or contractile proteins; six channel proteins; four prostaglandin synthesis enzymes; 12 endocrine factors or their binding proteins; six receptors; 15 signaling molecules; eight transcription factors; three chromatin or DNA binding proteins; nine cytoskeletal proteins; seven cell surface or extracellular matrix proteins; and 11 enzymes for energy, nucleic acid, lipid, or steroid metabolism (Table 1). Although many of the above-mentioned categories also have genes that were down-regulated by CT, the most striking finding among the decreased genes are cell cycle regulators

(Table 1). We have verified the expression of bcl-xL, two GSTs, Cox 1 and 2, Hsp27, cyclin D2, cyclin B1, and proliferating cell nuclear antigen at the protein level by Western blot analyses using commercially available antibodies. Those have been verified by Western blot show consistent results with microarray or RT-PCR analyses in induction or reduction (Fig. 8). The gene array data suggest that CT induces multiple changes at the gene expression level. A part of these changes probably contribute to the observed cytoprotection as reported here.

Induction of Bcl-xL in Absence of Elevation of Bcl-2 or Proapoptotic Factors. The prosurvival members of the bcl-xL family can protect cells from apoptosis in various experimental systems. An increase in the protein level of bcl-xL could explain the cytoprotection induced by CT pretreatment. To determine the correlation between bcl-xL induction and inhibition of apoptosis, we have measured the dose response and time course of bcl-xL induction. An elevation of bcl-xL protein was observed with 24-h treatment of CT at the concentration of 0.1 μM and the elevation reached its highest level with 1.0 μM CT (Fig. 9A). With 1.0 μM CT treatment, the elevation was significant at 4 h, reached the highest induction at 8 h, and remained at the highest level of induction throughout 72 h (Fig. 9B). Treatment with MF abolished induction of bcl-xL by CT (Fig. 9C). The dose response, time course, and the impact of MF studies suggest that bcl-xL induction correlates well with the cytoprotective effect of CT.

Previous studies found that treatment with Dox can change the level of bcl-xL protein (Negoro et al., 2001), posing the question of whether induction of bcl-xL indeed contributes to the observed cytoprotective effect of CT. We determined the levels of bcl-xL induction by CT with or without

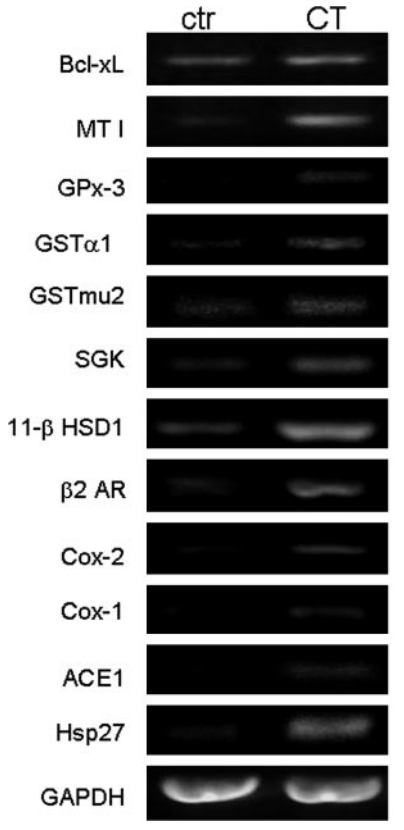

Fig. 7. RT-PCR verification of increased expression of antiapoptosis, antioxidant, detoxification, and other genes identified by microarray analyses. Cardiomyocytes were treated with 1 μM CT for 24 h, and total RNA (2 μg) was used for reverse transcription and PCR reaction with primer pairs designed specifically for the metallothionein-I (MT I), glutathione peroxidase-3 (GPx-3), GSTα1, GSTmu2, SGK, 11β-HSD1, β2-AR, Cox-2, Cox-1, ACE1, Hsp27, or glyceraldehyde-3-phosphate dehydrogenase (GADPH). The PCR products were detected by ethidium bromide staining after agarose gel electrophoresis. Alpha Innotech (San Leandro, CA) Image system was used to acquire the images using Adobe Photoshop software.

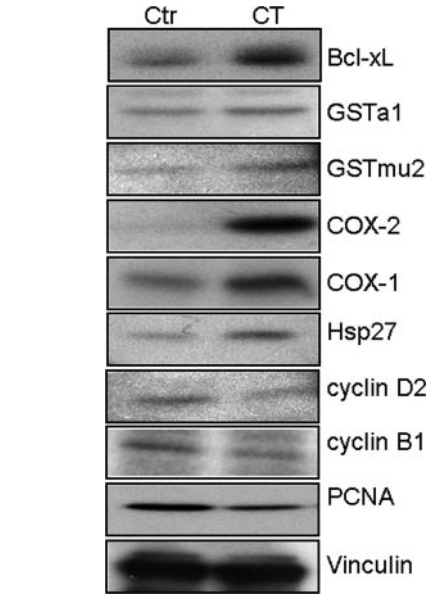

Fig. 8. Protein level verification of a fraction of genes identified by microarray. Cardiomyocytes were treated with 1 μM CT for 24 h and cell lysates were used for Western blot analyses (20 μg of protein/lane) as described under *Materials and Methods*. Vinculin was used as a loading control.

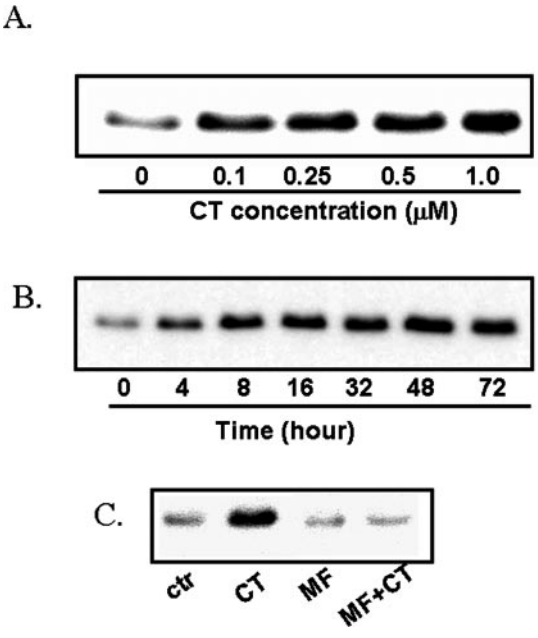

Fig. 9. CT dose- and time-dependent induction of Bcl-xL protein. Cardiomyocytes were treated with various doses for 24 h (A) or were treated with 1 μM CT for indicated time (B) or 24 h (C). MF at 1 μM dose was added to cells 30 min before addition of 1 μM CT (C). Cells were harvested for Western blot (20 μg of protein/lane) to measure for levels of bcl-xL as described under *Materials and Methods*.

Dox treatment. Figure 10 shows that although the induction of bcl-xL by CT is profound, Dox did not seem to alter the level of bcl-xL significantly in our experimental system within the time frame tested (24 h).

We have used stringent conditions to select for genes that were up- or down-regulated by CT treatment during microarray analyses. Target measurements of genes in the bcl-2 family allow us to determine the importance of bcl-xL elevation in CT-induced cytoprotection. Bcl-2 is another prosurvival factor, overexpression of which can protect cells from undergoing apoptosis. Measurement of bcl-2 protein revealed that CT or Dox did not induce significant changes in the level of bcl-2 protein (Fig. 10). Bcl-xL can dimerize with the proapoptotic factors bax and bak and prevent these proapoptotic factors from releasing mitochondrial cytochrome *c*. Bad, another proapoptotic factor, can inhibit the action of bcl-xL. Down-regulation of these proapoptotic factors could contribute to cytoprotection. To test this possibility, we have determined the level of bax, bak, and bad proteins in CT-treated cells with or without Dox treatment. The results show that CT or Dox treatment did not seem to alter the level of these proapoptotic protein factors within the time frame tested (Fig. 10).

To determine the contribution of bcl-xL induction in CT-induced cytoprotection, we have used siRNA to inhibit the expression of bcl-xL. Measurements of bcl-xL level after transfecting a combination of two siRNAs showed the retardation of bcl-xL induction by CT treatment (Fig. 11A). Measurements of caspase-3 activity at 16 h after Dox treatment indicated that bcl-xL siRNA abolished CT-mediated cytoprotection. Scoring the percentages of cells detached or showing nuclear condensation or nuclear fragmentation at 24 h after Dox treatment revealed that bcl-xL siRNAs partially reversed the cytoprotective effect of CT (Fig. 11, B and C). These data suggest that induction of bcl-xL contributes to the cytoprotective effect of CT.

Discussion

This study revealed that CT inhibits apoptotic-like cell death induced by Dox in primary cultured cardiomyocytes. The dose range found to inhibit cell death in this study is 0.1 to 100 μM. The lowest dose tested here (i.e., 0.1 μM or 3.5 μg/dl) is related to the basal level of cortisol in the circulating system of humans (2–5 μg/dl). The concentration of CT relevant to the circulating level of cortisol in human during stress (0.7–1 μM) seemed to be optimal in inducing cytoprotection. Therefore, this finding may contribute to understanding the physiological impact of stress on the heart in humans.

Recent studies have demonstrated the presence of apoptotic cells in biopsy samples of failing human hearts and in the myocardium of experimental animals with failing hearts (Kang and Izumo, 2000; Chen and Tu, 2002). There is evidence that inhibiting apoptosis may alleviate certain clinical manifestations of heart failure in experimental animals (Feuerstein et al., 1998; Ma et al., 1999; Kotamraju et al., 2000). Dox is known to induce dilated cardiomyopathy. The presence of a large amount of apoptotic cells in the myocardium of Dox-treated patients has been traditionally thought

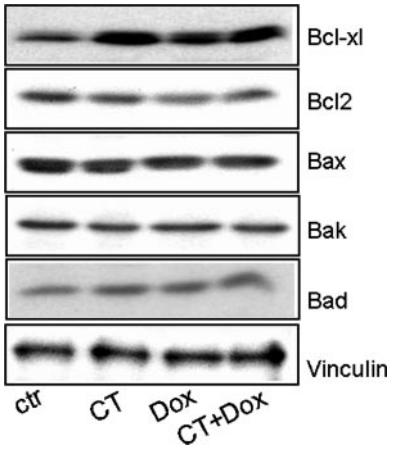

Fig. 10. Levels of Bcl-2, bax, bak, and bad in CT-treated cells with or without Dox treatment. Cardiomyocytes were cultured in DMEM containing 1 μM CT for 3 days. Cells were treated with Dox for 16 h and were harvested for measurement of levels of bcl-xL, bcl-2, bax, bak, and bad by Western blot as described under *Materials and Methods*. Blotting of vinculin shows equal loading of proteins between each lane (20 μg of protein/lane).

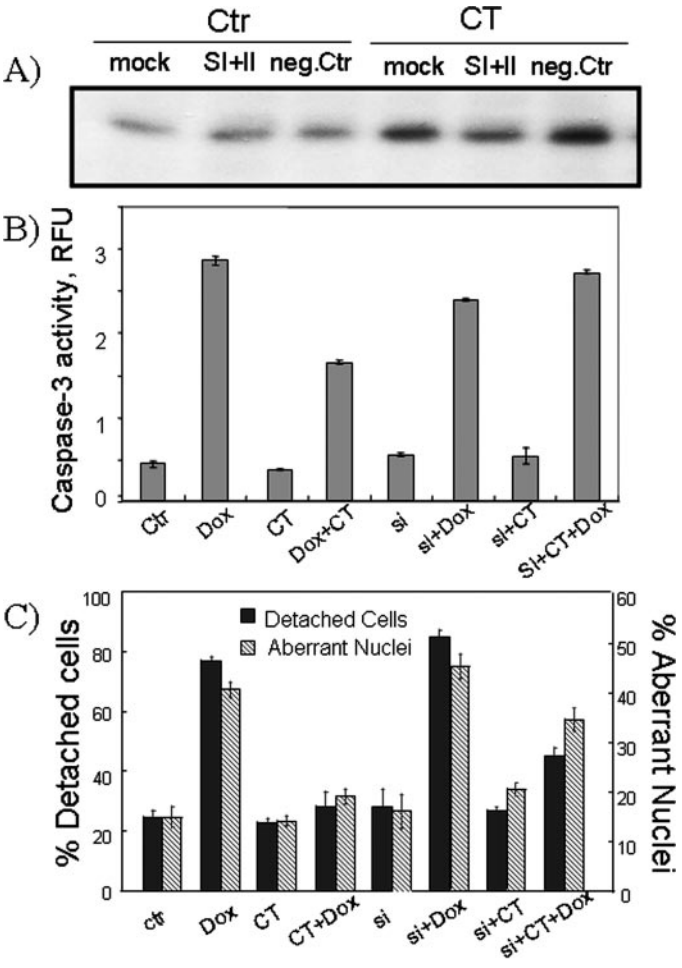

Fig. 11. Effect of bcl-xL siRNAs on CT-induced cytoprotection. Cardiomyocytes were transfected with two species of bcl-xL siRNA or a negative control. At 48 h after transfection, the cells were treated 8 h with 1 μM CT for measuring the level of bcl-xL protein by Western blot (A). After 24-h pretreatment of CT, cells were treated with 1 μM Dox for additional 16 h for measurement of caspase-3 activity (B). The cells were treated 24 h with 1 μM Dox for scoring the percentage of detached cells under a phase contrast microscope (C) or for scoring the percentage of nuclei showing condensation or fragmentation after propidium iodine staining under a fluorescent microscope (C) as described previously (Chen et al., 2002).

to contribute to the dilated cardiomyopathy and heart failure (Keizer et al., 1990; Singal et al., 2000). Therefore, inhibitors of apoptosis may provide hope for the prevention or treatment of Dox-induced cardiomyopathy.

One caveat is the potential difference of corticosteroid effects in vitro versus in vivo. The clinical impact of corticosteroids on the heart has been an issue under intensive debate (Ng and Celermajer, 2004). In general, physicians tend not to prescribe corticosteroids to patients with cardiovascular disease because of potential detrimental effects of the steroids on electrophysiology of the heart and on the vascular system. Earlier clinical observations indicate that administration of dexamethasone causes sudden cardiac arrhythmias (Schmidt et al., 1972; Rao et al., 1972). In addition, corticosteroids have been found to increase the peripheral vascular resistance and cause increases in blood pressure in a dose-dependent manner (Kelly et al., 1998; Whitworth et al., 2001). Prolonged overexposure to corticosteroids can cause Cushing's syndrome, a rare disease manifested by depression, osteoporosis, diabetes, and high blood pressure. In agreement with these unwanted effects, our microarray analyses show that CT induces the expression of β2-AR, which may affect the contractility and therefore arrhythmias of the heart. We also found that CT induces the expression of ACE1, which may result in an increased production of angiotensin II, a peptide known to contribute to cardiac hypertrophy and heart failure. The enzyme 11β-HSD converts 11-keto-steroids into active glucocorticoids and therefore amplifies the action of glucocorticoids. Despite these undesirable effects in vivo and in vitro, corticosteroids have been found to protect the heart from ischemia and reperfusion injury in animal models (Libby et al., 1973; Spath et al., 1974; Busuttil and George, 1978; Valen et al., 2000). Whether corticosteroids can initiate an antiapoptotic response in vivo in mediating the cardiac protective effect remains to be investigated.

The discovery of bcl-xL elevation provides one answer to the observed antiapoptotic effect of CT. The time course of bcl-xL elevation seems to be consistent with the long lag time (i.e., 8 h) required for cells to gain antiapoptotic ability and with the dependence of new protein synthesis for CT-induced cytoprotection. The balance of prosurvival factors versus proapoptotic factors in the bcl-2 family seems to be tipped toward the prosurvival side with the induction of bcl-xL, because no increase of proapoptotic factors bax, bak, and bad was observed with CT treatment. In certain experimental systems of chemical-induced apoptosis, increases in bax, bak, or bad have been observed. Bax, bak, or bad can form channels on the mitochondrial membrane for cytochrome *c* release when levels of these proapoptotic proteins are elevated or when they escape from the surveillance of their inhibitors, such as bcl-2 and bcl-xL. With Dox treatment alone, we did not observe an increase in the levels of bax, bak, or bad (Fig. 10). However a loss of mitochondrial cytochrome *c* was observed with Dox treatment (Fig. 3B), suggesting the possibility of mitochondrial membrane permeability transition in mediating cytochrome *c* release. Dox has been shown to produce reactive oxygen species (Doroshow and Davies, 1986; Keizer et al., 1990; Singal et al., 2000). Oxidants can induce mitochondrial membrane permeability transition, which is typically triggered by increases in cytosolic Ca^{2+} (Takeyama et al., 1993; Kuwana and Newmeyer, 2003). The endoplasmic reticulum (ER) plays a critical role in regulating the concentration of cytosolic Ca^{2+}. Recent evidence indicates that bcl-2 regulates the level of cytosolic Ca^{2+} through its ER localization (Kuwana and Newmeyer, 2003; Annis et al., 2004). Bcl-xL has also been found to locate in the ER in addition to its mitochondrial and cytosolic distribution (Annis et al., 2004). This suggests the possibility that bcl-xL may prevent apoptosis through inhibiting mitochondrial membrane permeability transition. However, we cannot exclude the possibility that Dox, without increasing the level of bax, bak, or bad, inactivates the surveillance of bax, bak, or bad, causing cytochrome *c* release through formation of mitochondrial membrane channels. CT enhances the surveillance by inducing bcl-xL, which inhibits the formation of mitochondrial cytochrome *c* release channel by bax, bak, and bad. Regardless, inhibiting the expression of bcl-xL using siRNAs proved the role of bcl-xL in the CT-induced antiapoptotic effect. The bcl-xL gene has been shown to be induced by a number of stimuli, such as UV irradiation, cytokines, and chemical stress (Grad et al., 2000). The elevated expression of bcl-xL can be regulated at transcriptional levels. The promoter region of the bcl-xL gene contains consensus-binding sites for Rel/nuclear factor-κB, Ets, and signal transducer and activator of transcription transcription factors. There is evidence that GR transcription factor can cross-talk with STAT-3 in regulating bcl-xL gene expression (Takeda et al., 1998).

Microarray analyses indicated that CT induces a multitude of changes at the gene expression level. Transcriptional regulation has been a main feature studied in the biology of corticosteroids (Karin, 1998; Adcock, 2001). Upon binding to corticosteroids, GR transforms from a silent to an active transcription factor. GR forms a homodimer that binds to the glucocorticoid response element (GRE) in the promoter region of target genes, resulting in transcriptional activation of these genes. Metallothionein I, a metal binding protein that has been shown to function as an antioxidant and protect cardiomyocytes from Dox-induced toxicity in vitro and in vivo (Kang, 1999; Sun et al., 2001), contains GRE in its promoter (Karin, 1998). Consistent with the literature, CT indeed induced the expression of metallothionein I in cardiomyocytes as indicated in our microarray and RT-PCR analysis. In addition to activating the transcription of genes containing the GRE in their promoter, corticosteroids have been shown to regulate transcription through chromatin remodeling and to repress transcription of genes containing a negative GRE *cis*-element in their promoters (Bamberger et al., 1996; Adcock, 2001; Deroo and Archer, 2001). CT can also bind to an orphan receptor, the pregnane X receptor (PXR) (Xie and Evans, 2001). Activation of PXR composes a novel steroid signaling and transcriptional regulation pathway that is distinct from the classic glucocorticoid receptor-mediated pathways. PXR knockout mice are hypersensitive to the toxicity of xenobiotics (Xie and Evans, 2001), suggesting a role of PXR in cytoprotection. These pieces of evidence in conjunction with our microarray data suggest that CT treatment can reprogram the gene expression profile in cardiomyocytes. Although induction of bcl-xL may contribute to cell survival, it seems unlikely that the observed cytoprotection induced by CT in cardiomyocytes is associated with one gene not the others. Changes in 1.7% of genes from the cardiomyocyte genome depict the state of CT-treated cells.

Acknowledgments

We thank Amber May in the Genomics Core facility of Arizona Cancer Center and Southwest Environmental Health Sciences Center (ES06694) for microarray analyses.

References

Adcock IM (2001) Glucocorticoid-regulated transcription factors. *Pulm Pharmacol Ther* **14:**211–219.

Angelucci L (2000) The glucocorticoid hormone: from pedestal to dust and back. *Eur J Pharmacol* **405:**139–147.

Annis MG, Yethon JA, Leber B, and Andrews DW (2004) There is more to life and death than mitochondria: Bcl-2 proteins at the endoplasmic reticulum. *Biochim Biophys Acta* **1644:**115–123.

Bamberger CM, Schulte HM, and Chrousos GP (1996) Molecular determinants of glucocorticoid receptor function and tissue sensitivity to glucocorticoids. *Endocr Rev* **17:**245–261.

Busuttil RW and George WJ (1978) Protective action of methylprednisolone on the isolated perfused rat heart following severe hypoxia. *Proc Soc Exp Biol Med* **157:**580–583.

Cadepond F, Ulmann A, and Baulieu EE (1997) RU486 (mifepristone): mechanisms of action and clinical uses. *Annu Rev Med* **48:**129–156.

Chen Q, Fischer A, Reagan JD, Yan LJ, and Ames BN (1995) Oxidative DNA damage and senescence of human diploid fibroblast cells. *Proc Natl Acad Sci USA* **92:**4337–4341.

Chen QM, Merrett JB, Dilley T, and Purdom S (2002) Down regulation of p53 with HPV E6 delays and modifies cell death in oxidant response of human diploid fibroblasts: an apoptosis-like cell death associated with mitosis. *Oncogene* **21:**5313–5324.

Chen Q and Tu V (2002) Apoptosis and heart failure: mechanisms and therapeutic implications. *Am J Cardiovasc Drugs* **2:**43–57.

Coronella-Wood J, Terrand J, Sun H, and Chen Q (2004) c-Fos phosphorylation induced by H_2O_2 prevents proteosomal degradation of c-Fos in cardiomyocytes. *J Biol Chem* **279:**33567–33574.

De Windt LJ, Lim HW, Taigen T, Wencker D, Condorelli G, Dorn GW 2nd, Kitsis RN, and Molkentin JD (2000) Calcineurin-mediated hypertrophy protects cardiomyocytes from apoptosis in vitro and in vivo: an apoptosis-independent model of dilated heart failure. *Circ Res* **86:**255–263.

Deroo BJ and Archer TK (2001) Glucocorticoid receptor-mediated chromatin remodeling in vivo. *Oncogene* **20:**3039–3046.

Doroshow JH and Davies KJ (1986) Redox cycling of anthracyclines by cardiac mitochondria. II. Formation of superoxide anion, hydrogen peroxide and hydroxyl radical. *J Biol Chem* **261:**3068–3074.

Feuerstein G, Yue TL, Ma X, and Ruffolo RR (1998) Novel mechanisms in the treatment of heart failure: inhibition of oxygen radicals and apoptosis by carvedilol. *Prog Cardiovasc Dis* **41:**17–24.

Grad JM, Zeng XR, and Boise LH (2000) Regulation of Bcl-xL: a little bit of this and a little bit of STAT. *Curr Opin Oncol* **12:**543–549.

Guyton AC and Hall JE (2000) The adrenocortical hormones, in *Textbook of Medical Physiology*, pp 869–883, W. B. Saunders Company, Philadelphia.

Hickson-Bick DL, Sparagna GC, Buja LM, and McMillin JB (2002) Palmitate-induced apoptosis in neonatal cardiomyocytes is not dependent on the generation of ROS. *Am J Physiol* **282:**H656–H664.

Kang PM and Izumo S (2000) Apoptosis and heart failure: a critical review of the literature. *Circ Res* **86:**1107–1113.

Kang YJ (1999) The antioxidant function of metallothionein in the heart. *Exp Biol Med* **222:**263–273.

Karin M (1998) New twists in gene regulation by glucocorticoid receptor: is DNA binding dispensable? *Cell* **93:**487–490.

Keizer HG, Pinedo HM, Schuurhuis GJ, and Joenje H (1990) Doxorubicin (adriamycin): a critical review of free radical-dependent mechanisms of cytotoxicity. *Pharmacol Ther* **47:**219–231.

Kelly JJ, Mangos G, Williamson PM, and Whitworth JA (1998) Cortisol and hypertension. *Clin Exp Pharmacol Physiol* **25 (Suppl):**S51–S56.

Kotamraju S, Konorev EA, Joseph J, and Kalyanaraman B (2000) Doxorubicin-induced apoptosis in endothelial cells and cardiomyocytes is ameliorated by nitrone spin traps and ebselen. Role of reactive oxygen and nitrogen species. *J Biol Chem* **275:**33585–33592.

Kuwana T and Newmeyer DD (2003) Bcl-2-family proteins and the role of mitochondria in apoptosis. *Curr Opin Cell Biol* **15:**691–699.

Layne E (1957) Spectrophotometric and turbidimetric methods for measuring proteins. *Methods Enzymol* **3:**447–454.

Libby P, Maroko PR, Bloor CM, Sobel BE, and Braunwald E (1973) Reduction of experimental myocardial infarct size by corticosteroid administration. *J Clin Investig* **52:**599–607.

Ma XL, Kumar S, Gao F, Louden CS, Lopez BL, Christopher TA, Wang C, Lee JC, Feuerstein GZ, and Yue TL (1999) Inhibition of p38 mitogen-activated protein kinase decreases cardiomyocyte apoptosis and improves cardiac function after myocardial ischemia and reperfusion. *Circulation* **99:**1685–1691.

Negoro S, Oh H, Tone E, Kunisada K, Fujio Y, Walsh K, Kishimoto T, and Yamauchi-Takihara K (2001) Glycoprotein 130 regulates cardiac myocyte survival in doxorubicin-induced apoptosis through phosphatidylinositol 3-kinase/Akt phosphorylation and Bcl-xL/caspase-3 interaction. *Circulation* **103:**555–561.

Ng MK and Celermajer DS (2004) Glucocorticoid treatment and cardiovascular disease. *Heart* **90:**829–830.

Rao G, Zikria EA, Miller WH, Samadani SR, and Ford WB (1972) Cardiac arrhythmias after dexamethasone. *J Am Med Assoc* **222:**1185.

Schmidt GB, Meier MA, and Sadove MS (1972) Sudden appearance of cardiac arrhythmias after dexamethasone. *J Am Med Assoc* **221:**1402–1404.

Singal PK, Li T, Kumar D, Danelisen I, and Iliskovic N (2000) Adriamycin-induced heart failure: mechanism and modulation. *Mol Cell Biochem* **207:**77–86.

Spath JA Jr, Lane DL, and Lefer AM (1974) Protective action of methylprednisolone on the myocardium during experimental myocardial ischemia in the cat. *Circ Res* **35:**44–51.

Sun X, Zhou Z, and Kang YJ (2001) Attenuation of doxorubicin chronic toxicity in metallothionein-overexpressing transgenic mouse heart. *Cancer Res* **61:**3382–3387.

Takeda T, Kurachi H, Yamamoto T, Nishio Y, Nakatsuji Y, Morishige K, Miyake A, and Murata Y (1998) Crosstalk between the interleukin-6 (IL-6)-JAK-STAT and the glucocorticoid-nuclear receptor pathway: synergistic activation of IL-6 response element by IL-6 and glucocorticoid. *J Endocrinol* **159:**323–330.

Takeyama N, Matsuo N, and Tanaka T (1993) Oxidative damage to mitochondria is mediated by the Ca^{2+}-dependent inner-membrane permeability transition. *Biochem J* **294:**719–725.

Valen G, Kawakami T, Tahepold P, Dumitrescu A, Lowbeer C, and Vaage J (2000) Glucocorticoid pretreatment protects cardiac function and induces cardiac heat shock protein 72. *Am J Physiol* **279:**H836–H843.

Whitworth JA, Schyvens CG, Zhang Y, Mangos GJ, and Kelly JJ (2001) Glucocorticoid-induced hypertension: from mouse to man. *Clin Exp Pharmacol Physiol* **28:**993–996.

Xie W and Evans RM (2001) Orphan nuclear receptors: the exotics of xenobiotics. *J Biol Chem* **276:**37739–37742.

Yudt MR and Cidlowski JA (2002) The glucocorticoid receptor: coding a diversity of proteins and responses through a single gene. *Mol Endocrinol* **16:**1719–1726.

Address correspondence to: Dr. Qin M. Chen, Department of Pharmacology, 1501 N. Campbell Ave., University of Arizona, Tucson, AZ 85724. E-mail: qchen@email.arizona.edu